A&A 519, A101 (2010)
DOI: 10.1051/0004-6361/200811026

Astronomy & Astrophysics

Rotation and lithium abundance of solar-analog stars

Theoretical analysis of observations

J. D. do Nascimento Jr, J. S. da Costa, and J. R. De Medeiros

Departamento de Física Teórica e Experimental, Universidade Federal do Rio Grande do Norte, 59072-970 Natal, RN, Brazil
e-mail: dias@dfte.ufrn.br

Received 24 September 2008 / Accepted 27 May 2010

ABSTRACT

Context. Rotational velocity, lithium abundance, and the mass depth of the outer convective zone are key parameters in the study of the processes at work in the stellar interior, in particular when examining the poorly understood processes operating in the interior of solar–analog stars.
Aims. We investigate whether the large dispersion in the observed lithium abundances of solar-analog stars can be explained by the depth behavior of the outer convective zone masses, within the framework of the standard convection model based on the local mixing-length theory. We also analyze the link between rotation and lithium abundance in solar-analog stars.
Methods. We computed a new extensive grid of stellar evolutionary models, applicable to solar-analog stars, for a finely discretized set of mass and metallicity. From these models, the stellar mass, age, and mass depth of the outer convective zone were estimated for 117 solar-analog stars, using Teff and [Fe/H] available in the literature, and the new HIPPARCOS trigonometric parallax measurements.
Results. We determine the age and mass of the outer convective zone for a bona fide sample of 117 solar-analog stars. No significant one-to-one correlation is found between the computed convection zone mass and published lithium abundance, indicating that the large A(Li) dispersion in solar analogs cannot be explained by the classical framework of envelope convective mixing coupled with lithium depletion at the bottom of the convection zone.
Conclusions. These results illustrate the need for an extra-mixing process to explain lithium behavior in solar-analog stars, such as, shear mixing caused by differential rotation. To derive a more realistic definition of solar-analog stars, as well as solar-twin stars, it seems important to consider the inner physical properties of stars, such as convection, hence rotation and magnetic properties.

Key words. Hertzsprung-Russell and C-M diagrams – stars: rotation – stars: abundances – stars: fundamental parameters

1. Introduction

The evolutionary behavior of lithium abundance and rotation, and the convective properties of stars depend strongly on stellar mass. The genesis of this dependence is of obvious interest in stellar astrophysics, in particular for the study of solar-analog stars, but very little is known about this subject. For the convective properties, perhaps the foremost difficulty lies in the criteria used to the define solar-analog or solar twin, stars that are spectroscopically and photometrically identical to the Sun (Cayrel de Strobel 1996). Different studies have suggested that the Sun could be: (i) an abnormally slow rotator; and (ii) lithium-poor by a factor of 10 (Lambert & Reddy 2004) relative to similar solar-type disk stars, which raises the question of whether there is anything unusual about the solar rotation rate and Li abundance? King (2005), Takeda et al. (2007), Meléndez and Ramirez (2007) demostrated that, at least in terms of its lithium content, the Sun is a normal star at its present evolutionary stage. In spite of dozens of stars having been classified as solar-analogs (e.g: Takeda et al. 2007), only three solar twins are known: 18 Sco (Porto de Mello & da Silva 1997), HD 98618 (Meléndez et al. 2006), and HIP 100963 (Takeda et al. 2007), all of witch have a Li abundance higher than the solar value by a factor of beetwen 3 and 6. For instance, spectroscopic analysis of the solar twin 18 Sco by Porto de Mello and Da Silva (1997) demostrated that the atmospheric parameters, chromospheric activity, and UBV colors of this object are indistinguishable from solar values, but that the system has an excess of Sc, V, and heavier elements. In addition, Meléndez and Ramirez (2007) presented data for two solar twins of low Li abundance (HIP 56948 and HIP 73815), pointing to a factor of about 200 in Li depletion relative to that found in meteorites. This finding clearly contradicts some standard model predictions (models without rotation at any depth with the hypothesis that stellar convective regions are instantly mixed and that no chemical transport occurs in the radiative regions) and represents a long-standing puzzle in stellar astrophysics. Pasquini et al. (2008) showed that five bona-fide main-sequence stars of the open cluster M 67 are potential solar-twins. These stars have low Li content, comparable to the photospheric solar value, probably indicating similar mixing evolution. In addition, these authors confirmed the presence of a large Li spread among the solar-type stars of M 67, showing for the first time that extra Li depletion appears only in stars cooler than 6000 K. This behavior indicates that these stars very likely experience a depletion in their Li during the main sequence (MS) stage, although their convective zones do not reach sufficiently deep into the stellar interior to meet the zone of Li destruction. The scatter in Li abundance in the solar cluster M 67 by a factor of ∼10 around the solar-age (Spite et al. 1987; García López et al. 1988) is a solid example of the disagreement between observations and the theoretical predictions of standard models, implying that depletion must be affected by an additional parameter

besides mass, age, and chemical composition (Pasquini et al. 1997; Jones et al. 1999; Randich et al. 2006).

In the present work, we investigate the influence of mass, $T_{\rm eff}$, age, and mass depth of the outer convective zone on the behavior of Li abundance and rotational velocity in solar-analog stars and twins. A close examination of some stellar parameters (stellar mass and convection-zone mass deepening) may shed new light on the lithium behavior in this family of stars.

We redetermine the evolutionary status and individual masses for a sample of 117 solar-analogs, using HIPPARCOS parallaxes and by comparing the observational Hertzsprung-Russell diagram with evolutionary tracks, following the procedure described in Sect. 2. As in do Nascimento et al. (2009), we show that it is possible to precisely determine the mass and age of solar analogs and twins using evolutionary models calibrated to reproduce solar luminosity, radius, and Li depletion. The characteristics of the working sample are also described in Sect. 2. In Sect. 3, the main lithium and rotation features are presented, with an analysis of the influence of mass and convection zone depth on these parameters. Finally, the main conclusions are outlined in Sect. 4.

2. Stellar evolutionary models and working sample

In the next sections, we discuss about the stellar evolutionary models ingredients and the characteristics of the observational data used in this study.

2.1. Stellar evolutionary models

For the purposes of the present study, evolutionary tracks were computed with the Toulouse-Geneva stellar evolution code TGEC (Hui-Bon-Hoa 2007). Details about the underlying physics of these models can be found in Richard et al. (1996), do Nascimento et al. (2000), Hui-Bon-Hoa (2007), and do Nascimento et al. (2009). Here, we provide a short description of the main physical stellar model ingredients.

Input physics

We used the OPAL2001 equation of state by Rogers and Nayfonov (2002) and the radiative opacities by Iglesias & Rogers (1996), in addition to the low temperature atomic and molecular opacities by Alexander & Ferguson (1994). The nuclear reactions are from the analytical formulae of the NACRE (Angulo et al. 1999) compilation, taking into account the three *pp* chains and the CNO tricycle, with the Bahcall & Pinsonneault (1992) screening routine. Convection is treated according to the Böhm-Vitense (1958) formalism of the mixing-length theory with $\alpha_{\rm p} = l/H_{\rm p} = 1.756515$. For the atmosphere, we used a grey atmosphere following the Eddington relation. The abundance variations of the following chemical species were individually computed in the stellar evolution code: H, He, C, N, O, Ne, and Mg. The heavier elements were gathered in Z. The initial composition followed the Grevesse and Noels (1993) mixture, with initial helium abundance $Y_{\rm ini} = 0.270$. All models included gravitational settling with diffusion coefficients computed as in Paquette et al. (1986). Radiative accelerations were not computed here, as we only focus on solar-type stars whose effects are negligible.

Our model grid includes 17 mass tracks spanning the mass range from 0.70 to 1.1 $M_{\odot}$ for four different metallicities, ([Fe/H] = 0.15, 0.0, –0.20 and –0.40). The evolution was followed from the zero-age main sequence (ZAMS) to the end of hydrogen exhaustion in the core. Evolution calculations were computed with a short step to match the effective solar temperature observed and luminosity at the solar age. The model calibration method was based on Richard et al. (1996), as follows: for a 1.00 $M_{\odot}$ star, we calibrated the mixing-length parameter (α_p) and initial helium abundance ($Y_{\rm ini}$) to match the observed solar luminosity and radius at solar age. The observed values that we used were those obtained by Richard et al. (2004): $L_{\odot} = 3.8515 \pm 0.0055 \times 10^{33}$ erg s^{-1}, $R_{\odot} = 6.95749 \pm 0.00241 \times 10^{10}$ cm and $Age_{\odot} = 4.57 \pm 0.02$ Gyr. For our best solar model, we obtained $L = 3.8541 \times 10^{33}$ erg s^{-1} and $R = 6.95743 \times 10^{10}$ cm at age = 4.57 Gyr. The input parameters for the other masses were the same as those of the 1.00 $M_{\odot}$ model. To verify model deviations in the mass determination, we compared the evolutionary tracks computed of this study with those used by Takeda et al. (2007) (evolutionary tracks from Girardi et al. 2000). Both evolutionary tracks are of solar metallicity, with stellar masses by Takeda et al. (2007) covering only three values, namely 0.9, 1.0, and 1.1 $M_{\odot}$.

2.2. Working sample

Our analysis is based on the observational data obtained by Takeda et al. (2007) for a sample of 117 field solar-analog stars selected from the HIPPARCOS catalog (ESA 1997), according to the criteria $V < 8.5$, $0.62 \leq B - V \leq 0.67$ and $4.5 \leq M_{\rm V} \leq 5.1$. These authors determined lithium abundance from the resonance Li I 6707.8 Å doublet, with associated errors around 0.1 dex, (caused by uncertainties in atmospheric parameters). Rotational velocities were obtained from Nordström et al. (2004) and Holmberg et al. (2007), with typical errors of about 1 km s^{-1}. The reader is referred to these papers for observational procedures, data reduction, and error analysis. We also re-examined the kinematic properties of each star based on the proper motion data taken from the HIPPARCOS catalog and radial velocity measurements, confirming the result found by Takeda et al. (2007) that all 117 field solar-analog stars selected belong to the normal thin-disk population.

Following the procedure of do Nascimento et al. (2000), we used the new HIPPARCOS trigonometric parallax measurements to precisely locate the objects in the HR diagram. Intrinsic absolute magnitudes $M_{\rm V}$ were derived from the parallaxes, the V magnitudes also being taken from HIPPARCOS. Stellar luminosity and the associated error were computed from the σ error in the parallax. The uncertainties in luminosity, ±0.1, have an effect of ±0.03 in the determination of the masses. Figure 1 shows the HR diagram with the evolutionary tracks computed for four different metallicity values ([Fe/H] = 0.15, 0.0, –0.20, and –0.40), which encompasses most of the stars contained in the present working sample.

Table 1 shows a comparison between the theoretical luminosities, effective temperatures, and ages of the Toulouse-Geneve evolution code (TGEC) and Girardi et al. (2000) to examine the difference around the observed effective solar temperature and luminosity. Our values for age, luminosity, and effective temperature are in close agreement with both those of Richard et al. (1996) and helioseismological predictions. Some discrepancies were found between our values and those of Girardi et al. (2000).

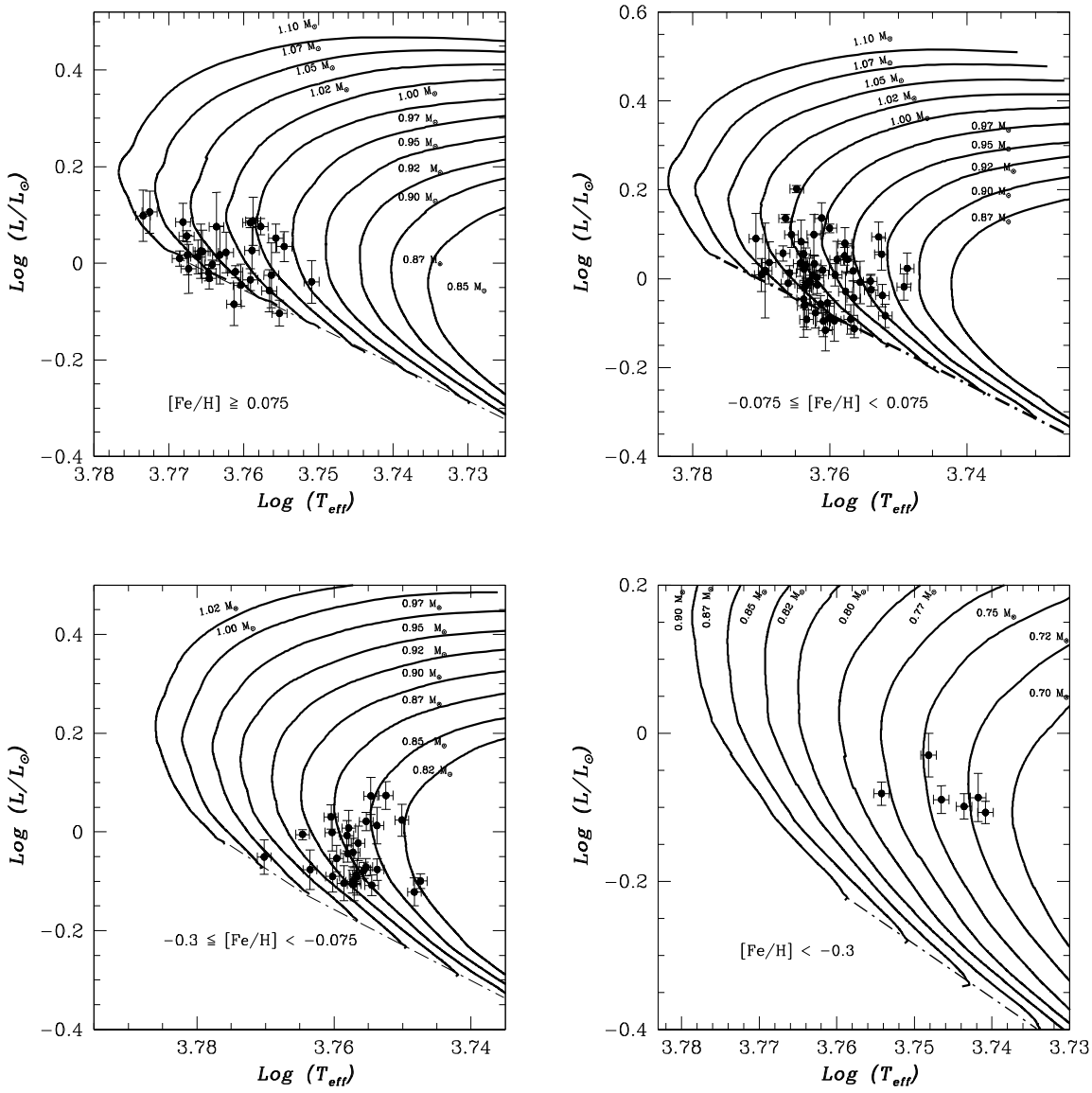

Fig. 1. The distribution of the analog sample stars in the Hertzsprung-Russell diagram. Luminosities and related errors have been derived from the Hipparcos parallaxes. The typical error in $T_{\rm eff}$ is ± 12 K (Takeda et al. 2007). Evolutionary tracks for [Fe/H] = 0.15, 0.0, –0.20, and –0.40 and stellar masses spanning the 0.70 to 1.1 $M_{\odot}$ mass range.

Table 1. Comparison between effective temperature and luminosity at the solar age from the Toulouse-Geneve evolution code TGEC and Girardi et al. (2000).

Model	log L	log($T_{\rm eff}$)	Age
TGEC	–0.00033	3.76212	4.5767739×10^9
TGEC	0.00020	3.76215	4.5917307×10^9
Girardi et al.	–0.021	3.760	4.02403×10^9
Girardi et al.	0.023	3.762	5.20367×10^9

2.3. Mass, age, and convective mass determination

We computed a careful star-by-star model for each star in our sample, with metallicity that matching that observed for each solar analog. The errors in $T_{\rm eff}$, luminosity, and [Fe/H] correspond to a mean error of 0.05 $M_{\odot}$ in the mass. As a consistency check, a comparison between our mass determination and those obtained by Takeda et al. (2007) is shown in Fig. 2. Except for some minor discrepancies for stars with masses lower than 0.8 $M_{\odot}$ bacause of a lack of models used by Takeda et al. (2007), there is generally close agreement between the two sets of masses. Stellar ages were inferred simultaneously with the masses, from the evolutionary tracks. The error in these ages, due to the uncertainties in $T_{\rm eff}$, luminosity, and [Fe/H], is about 15% and depends strongly on parallax uncertainties. Stars located close to the ZAMS have much larger errors. A comparison with age values computed by Holmberg et al. (2007) and Takeda et al. (2007), again finds no significant differences. Figure 3 shows the convective zone mass deepening as a function of the decreasing effective temperature for 0.875, 0.900, 0.925, 0.950, 0.975, 1.00, 1.025, 1.050, 1.075, and 1.100 $M_{\odot}$, where only the solar metallicity models are considered. In this figure, solid circles represent the convection mass zone, $(1 - Mr/M_{*})$, for the stars of the present sample of solar-analogs, determined in the scope of this study, where we have taken into consideration the metallicity of each star. Solar-analog stars typically, exhibit outer convective zone

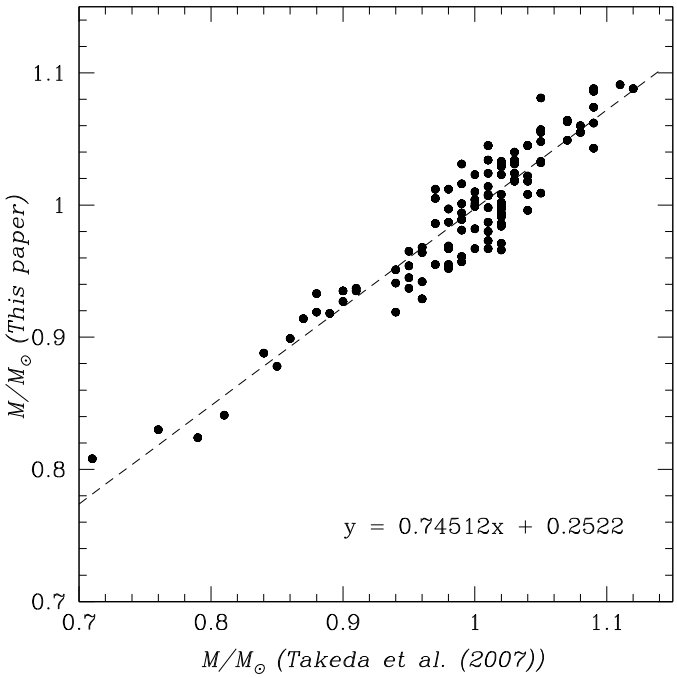

Fig. 2. Comparison between the mass determinations of this study, determined with the Toulouse-Geneva tracks and those computed by Takeda et al. (2007).

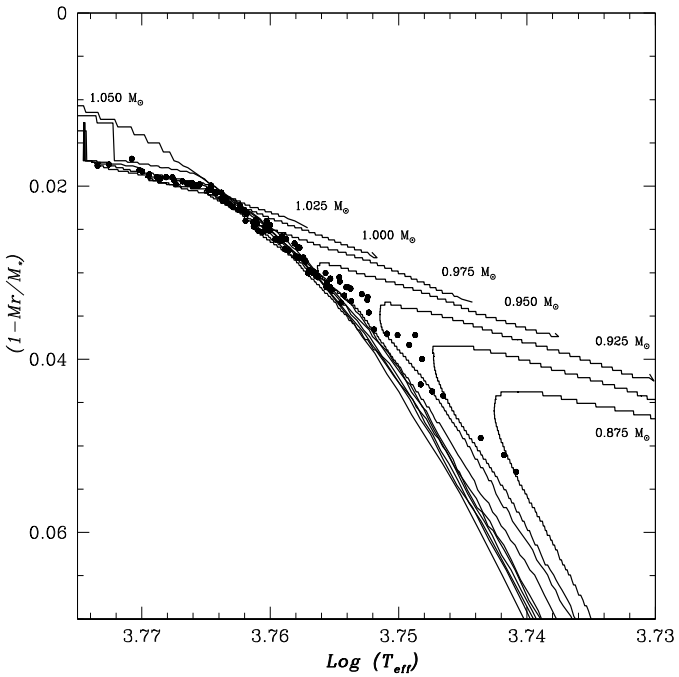

Fig. 3. Convective zone mass deepening as a function of decreasing effective temperature. Models for [Fe/H] = 0 and 0.875, 0.900, 0.925, 0.950, 0.975, 1.00, 1.025, 1.050, 1.075, and 1.100 $M_{\odot}$. The solid circle represents the surface convective mass determination of this study as a function of effective temperature for each star in the sample.

masses of around 0.02 $M_{\odot}$ (see $1 - Mr/M_{*}$ values in Table 2). A close look at Fig. 3 also indicates that the onset of convection zone deepening (in mass) is a strong function of stellar mass at the end of the pre-main-sequence phase. The depth of the outer convective zone in main-sequence stars depends primarily on mass. Deepening of the outer convective zone is also sensitive to metallicity. Quantitatively, a reduction in the initial metallicity $[Fe/H]_0$ from 0.0 to –0.4 should lead to a decrease in the outer convective zone ($1 - Mr/M_{*}$) from 0.022 to 0.004 at the Sun's age. Lithium data can be used to constrain the mass and metallicity-dependent process of the outer convective zone.

Lithium depletion in solar-twins caused by non-standard mixing is strongly mass-dependent (do Nascimento et al. 2009). A detailed comparison of the mass determinations of Takeda et al. (2007) and Nordström et al. (2004) reveals some discrepancies, such as HIP 45325. The masses obtained by Takeda et al. (2007) are systematically higher than the values obtained by Nordström et al. (2004). These discrepancies may be related to the completeness of the set of evolutionary models used by both authors. We recalculated as precisely as possible the mass of all sample stars. In this study, we used a set of homogeneous evolutionary tracks for main-sequence stars, computed for several masses and metal abundances, as discussed in Sect. 2.2. Mass determination was evaluated taking into account the metallicity effects, using the [Fe/H] values published by Takeda et al. (2007).

3. Results and discussion

We now discuss the relashionsip between the lithium abundance of solar-analog stars and their position in the HR diagram, verifying in particular the influence of the mass and outer convective zone depth on the letter. We consider in addition the rotational behavior of these stars. In addition, we show the important role of inner stellar properties in defining solar-analog stars and twins.

3.1. Main lithium features

Figure 4 shows the distribution of Li abundance for solar-analog stars in the HR diagram, with stars grouped into four different metallicity intervals, namely $[Fe/H] \geq 0.075$, $-0.075 \leq [Fe/H] < 0.075$, $-0.3 \leq [Fe/H] < -0.075$, and $[Fe/H] < -0.3$. The evolutionary tracks shown are those computed in the scope of the present work. A number of features can be observed in this figure: (i) Stars with masses <0.82 $M_{\odot}$ tend to have the lowest lithium content, most likely indicating that the same depletion level occurred in both the pre-main sequence and the early main sequence; (ii) stars with masses between 0.82 and 1.1 $M_{\odot}$ have a large scatter in their lithium content, possibly reflecting the different levels of lithium depletion. This star-to-star scatter in Li abundance was also observed in some solar-like field stars (Soderblom et al. 1993; Jones et al. 1999) and in members of the solar-age cluster M 67 (Pasquini et al. 2008).

The lithium scatter observed for solar-analogs indicates, in part, that these stars have also had different convection histories, which depend strongly on stellar mass, $T_{\rm eff}$, metallicity, and age. The classical interpretation is that Li has been destroyed in the stellar interior by proton-proton reactions at the bottom of the outer convection, i.e., at $T_{\rm bcz} > 2.5 \times 10^6$ K. Since the depth of the convection zone depends primarily on stellar mass, a correlation between Li abundance and mass is then expected for a given metallicity. This is observed in Figs. 5 and 6, which show the distribution of lithium abundance as a function of stellar mass and convection zone mass deepening ($1 - Mr/M_{*}$), respectively. In these figures, stars are grouped into the following metallicity ranges: open circles $[Fe/H] \geq 0.075$, squares $-0.075 \leq [Fe/H] < 0.075$, triangles $-0.3 \leq [Fe/H] < -0.075$, solid circles $[Fe/H] < -0.3$. The Sun, with $A(Li) = 1.1$ (Grevesse & Sauval 1998) and $(1 - Mr/M_{*}) = 0.021$ (see Table 2), is also displayed in both figures for comparative purposes.

Table 2. Parameters of the working sample.

HIP	HD	$\log(T_{\rm eff})$	$\log(L/L_{\odot})$	$M/M_{\odot}$	$(1-Mr/M_{*})$	$T_{\rm bcz}$ (10^6 K)	age (Gyr)	A(Li)	[Fe/H]	$v \sin i$
1499	1461	3.758	0.076 ± 0.017	1.03	0.023	2.25	3.34	<1.06	0.197	2
1598	1562	3.755	–0.071 ± 0.017	0.91	0.026	2.2	1.26	1.81	–0.272	3
1803	1835	3.765	–0.020 ± 0.016	1.09	0.019	2.19	0.94	2.65	0.239	7
4290	5294	3.757	–0.101 ± 0.023	0.97	0.025	2.23	0.93	2.18	–0.116	3
5176	6512	3.768	0.017 ± 0.041	1.06	0.018	1.98	5.76	1.89	0.185	3
6405	8262	3.758	–0.044 ± 0.018	0.96	0.025	2.21	2	1.71	–0.137	4
6455	8406	3.757	–0.106 ± 0.033	0.97	0.025	2.22	1.81	1.74	–0.088	2
7244	9472	3.76	–0.088 ± 0.027	1.0	0.023	2.21	1.24	2.29	–0.039	4
7585	9986	3.762	0.033 ± 0.018	1.02	0.021	2.17	2.84	1.84	0.074	1
7902	10145	3.749	–0.019 ± 0.030	0.97	0.03	2.36	1.33	<0.95	–0.008	1
7918	10307	3.766	0.135 ± 0.009	1.01	0.02	2.08	4.64	1.89	0.012	3
8486	11131	3.764	–0.046 ± 0.085	1.01	0.021	2.16	1.02	2.55	–0.061	4
9172	11926	3.761	–0.117 ± 0.045	1.03	0.022	2.22	0.86	2.5	0.063	5
9349	12264	3.762	0.007 ± 0.044	1.01	0.021	2.16	2.52	2.06	0.01	3
9519	12484	3.767	–0.011 ± 0.051	1.08	0.018	2.14	0.42	2.97	0.139	–
9829	12846	3.747	–0.090 ± 0.019	0.88	0.031	2.27	1.09	<0.91	–0.306	2
10321	13507	3.756	–0.113 ± 0.020	1.0	0.025	2.27	0.59	2.5	–0.005	3
11728	15632	3.757	–0.044 ± 0.039	0.99	0.026	2.27	2.8	<1.03	0.023	1
12067	15851	3.757	–0.057 ± 0.043	1.03	0.024	2.3	2.6	<1.27	0.202	1
14614	19518	3.758	0.008 ± 0.036	0.96	0.025	2.2	2.58	1.58	–0.122	3
14623	19632	3.759	–0.034 ± 0.023	1.03	0.023	2.26	1.61	2	0.122	4
15062	20065	3.759	–0.104 ± 0.036	0.92	0.025	2.16	1.35	2.02	–0.287	2
15442	20619	3.754	–0.108 ± 0.021	0.94	0.027	2.23	1.37	1.67	–0.188	3
16405	21774	3.759	0.087 ± 0.050	1.05	0.022	2.23	3.47	<1.2	0.263	1
17336	23052	3.754	–0.076 ± 0.022	0.94	0.027	2.24	2.58	<0.81	–0.126	1
18261	24552	3.769	0.036 ± 0.047	1.03	0.019	2.09	3.06	2.27	0.024	3
19793	26736	3.765	0.024 ± 0.044	1.07	0.018	2.13	1.63	2.53	0.187	6
19911	26990	3.754	0.013 ± 0.037	0.95	0.027	2.27	0.65	2.26	–0.127	5
19925	27063	3.761	–0.096 ± 0.034	1.02	0.022	2.18	3.26	1.61	0.071	2
20441	27685	3.761	–0.085 ± 0.044	1.05	0.022	2.22	1.44	2.28	0.13	3
20719	28068	3.766	0.025 ± 0.056	1.06	0.019	2.17	1.21	2.6	0.134	6
20741	28099	3.763	0.017 ± 0.060	1.06	0.02	2.19	1.38	2.41	0.163	4
20752	28192	3.773	0.106 ± 0.044	1.09	0.013	1.9	2.02	2.72	0.155	5
21165	27757	3.76	0.030 ± 0.025	0.95	0.024	2.16	2.65	1.61	–0.16	2
21172	28821	3.75	0.024 ± 0.032	0.94	0.03	2.33	1.37	< 0.96	–0.103	1
22203	30246	3.759	0.026 ± 0.047	1.04	0.023	2.27	0.95	2.3	0.133	3
23530	31864	3.748	–0.122 ± 0.028	0.9	0.031	2.29	1.28	<0.75	–0.238	–
25002	35041	3.758	–0.008 ± 0.030	0.98	0.024	2.23	0.78	2.38	–0.083	5
25414	35073	3.751	–0.038 ± 0.044	1.0	0.029	2.37	1.44	<1.1	0.097	1
25670	36152	3.76	–0.045 ± 0.043	1.01	0.023	2.18	3.98	<1.2	0.099	1
26381	37124	3.742	–0.087 ± 0.033	0.83	0.034	2.26	1.01	<0.66	–0.447	–
27435	38858	3.756	–0.078 ± 0.016	0.93	0.026	2.2	1.91	1.53	–0.215	3
29432	42618	3.757	–0.087 ± 0.017	0.95	0.026	2.22	2.79	1.06	–0.117	4
31965	47309	3.761	0.136 ± 0.035	1.0	0.023	2.16	4.64	1	0.048	3
32673	49178	3.758	–0.030 ± 0.045	1.0	0.025	2.24	3.41	<1.04	0.06	2
33932	49985	3.77	–0.051 ± 0.035	1.0	0.018	2.04	2.56	2.48	–0.118	4
35185	56202	3.763	–0.006 ± 0.052	1.02	0.021	2.18	0.67	2.71	–0.003	7
35265	56124	3.764	0.022 ± 0.025	1.0	0.021	2.12	2.82	2.01	–0.018	1
36512	59711	3.757	–0.042 ± 0.029	0.96	0.025	2.23	2.62	1.25	–0.091	2
38647	64324	3.757	–0.092 ± 0.033	1.0	0.025	2.26	1.01	2.13	0.01	3
38747	64942	3.764	–0.061 ± 0.047	1.05	0.02	2.18	0.66	2.75	0.065	6
38853	65080	3.771	0.090 ± 0.056	1.02	0.019	2.06	2.55	2.44	–0.052	1
39506	66573	3.748	–0.030 ± 0.029	0.81	0.03	2.13	1.28	<0.93	–0.62	2
39822	66171	3.76	–0.001 ± 0.037	0.93	0.024	2.15	3.28	<1.18	–0.218	2
40118	68017	3.744	–0.099 ± 0.017	0.84	0.033	2.26	0.98	<0.86	–0.42	2
40133	68168	3.756	0.052 ± 0.030	1.02	0.025	2.31	1.73	1.54	0.122	2
41184	70516	3.756	–0.025 ± 0.067	1.03	0.025	2.31	0.29	2.83	0.106	13
41526	71227	3.764	0.030 ± 0.039	1.0	0.021	2.13	2.64	2.03	–0.017	3
42333	73350	3.765	–0.032 ± 0.021	1.06	0.019	2.16	1.94	2.35	0.144	5
42575	73393	3.754	–0.026 ± 0.036	0.99	0.027	2.32	1.91	1.17	0.058	1
43297	75302	3.755	–0.104 ± 0.027	1.01	0.026	2.31	1.56	1.6	0.083	2
43557	75767	3.764	0.056 ± 0.025	0.98	0.021	2.11	4.18	1.5	–0.06	4
43726	76151	3.761	–0.018 ± 0.013	1.03	0.022	2.21	2.32	1.88	0.114	3
44324	77006	3.77	0.008 ± 0.037	1.03	0.019	2.07	2.76	2.41	–0.01	1
44997	78660	3.756	–0.009 ± 0.048	0.99	0.025	2.27	2.57	<1.24	0.044	2
45325	79282	3.773	0.098 ± 0.053	1.09	0.017	1.95	5.32	2.35	0.178	3

Table 2. continued.

HIP	HD	$\log(T_{\rm eff})$	$\log(L/L_{\odot})$	$M/M_{\odot}$	$(1 - Mr/M_{*})$	$T_{\rm bcz}$ (10^6 K)	age (Gyr)	A(Li)	[Fe/H]	$v \sin i$
46903	82460	3.759	–0.095 ± 0.046	0.99	0.023	2.21	1.88	2.02	–0.025	–
49580	87680	3.762	–0.077 ± 0.034	1.01	0.022	2.17	2.44	1.98	0.023	1
49586	87666	3.762	0.022 ± 0.042	1.05	0.02	2.09	4.77	<1.33	0.2	–
49728	88084	3.759	0.009 ± 0.025	0.97	0.024	2.19	3.43	<1.05	–0.068	3
49756	88072	3.757	0.043 ± 0.031	0.99	0.025	2.24	2.88	1.34	0.019	2
50505	89269	3.747	–0.100 ± 0.015	0.92	0.031	2.32	1.11	<0.92	–0.169	1
51178	90494	3.763	–0.077 ± 0.040	0.95	0.023	2.11	3.89	<1.22	–0.174	–
53721	95128	3.765	0.202 ± 0.008	1.0	0.021	2.11	3.68	1.75	–0.019	3
54375	96497	3.764	0.075 ± 0.071	1.06	0.02	2.19	1.44	2.44	0.136	6
55459	98618	3.764	0.034 ± 0.028	1.02	0.021	2.12	3.81	1.58	0.066	1
55868	99505	3.76	-0.091 ± 0.031	0.96	0.023	2.17	1.44	2.14	–0.148	4
56948	101364	3.762	0.099 ± 0.046	–	–	–	–	–	0.02	1
59589	106210	3.752	–0.038 ± 0.025	0.97	0.028	2.31	1.66	<1.21	–0.013	2
59610	106252	3.766	0.099 ± 0.029	0.99	0.021	2.09	4.39	1.62	–0.062	1
62175	110869	3.755	0.034 ± 0.031	1.02	0.026	2.35	1.02	1.83	0.133	1
62816	111938	3.764	–0.021 ± 0.044	1.03	0.021	2.16	2.26	2.16	0.062	4
63048	112257	3.752	0.055 ± 0.036	0.97	0.028	2.32	1.78	<1.11	–0.016	2
63636	113319	3.763	-0.092 ± 0.023	1.01	0.021	2.15	1.88	2.26	–0.01	4
64150	114174	3.758	0.051 ± 0.020	1.0	0.024	2.22	3.75	<1.04	0.054	3
64747	115349	3.757	–0.091 ± 0.037	0.94	0.025	2.19	2.76	<1.14	-0.178	2
70319	126053	3.754	-0.081 ± 0.016	0.89	0.027	2.18	2.27	1.09	–0.327	2
72604	131042	3.752	0.073 ± 0.028	0.94	0.028	2.27	1.9	<1.1	–0.142	1
73815	133600	3.764	0.083 ± 0.049	–	–	–	–	–	0.01	–
75676	138004	3.761	–0.057 ± 0.020	0.97	0.023	2.16	4.13	<1.07	–0.075	2
76114	138573	3.757	0.017 ± 0.023	0.97	0.028	2.3	2.34	0.91	-0.023	2
77749	142072	3.766	0.013 ± 0.035	1.09	0.018	2.17	0.97	2.7	0.223	7
78217	144061	3.76	–0.054 ± 0.027	0.94	0.024	2.15	1.99	1.89	–0.224	1
79672	146233	3.761	0.018 ± 0.011	1.01	0.022	2.17	3.3	1.63	0.039	3
85042	157347	3.754	–0.006 ± 0.014	0.98	0.027	2.29	2.62	<0.82	0.034	1
85810	159222	3.768	0.056 ± 0.011	1.06	0.019	2.09	3.89	2.05	0.149	3
88194	164595	3.755	0.021 ± 0.018	0.96	0.026	2.24	2.99	<0.83	–0.083	–
88945	166435	3.763	–0.013 ± 0.015	0.99	0.022	2.11	4.59	<1.1	–0.01	8
89282	167389	3.766	0.013 ± 0.017	1.02	0.019	2.1	2.09	2.45	–0.002	3
89474	168009	3.76	0.113 ± 0.010	0.99	0.023	2.16	4.41	<0.88	0.006	3
89912	168874	3.767	0.057 ± 0.017	1.05	0.019	2.15	0.93	2.69	0.041	7
90004	168746	3.749	0.023 ± 0.035	0.97	0.03	2.37	1.03	<1.17	–0.015	2
91287	171665	3.752	-0.084 ± 0.026	0.98	0.028	2.32	0.92	1.74	–0.007	2
96184	184403	3.768	0.085 ± 0.039	1.04	0.018	1.92	6.7	1.65	0.132	1
96395	185414	3.765	-0.005 ± 0.010	0.99	0.021	2.12	2.32	2.18	–0.1	1
96402	184768	3.753	0.094 ± 0.034	0.97	0.027	2.29	1.96	<1.11	–0.033	1
96901	186427	3.759	0.084 ± 0.010	1.01	0.024	2.22	3.29	<1.06	0.081	2
96948	186104	3.758	0.079 ± 0.037	1.01	0.024	2.24	2.52	1.52	0.07	2
97420	187237	3.762	0.002 ± 0.016	1.02	0.022	2.2	1.74	2.22	0.053	2
98921	190771	3.764	–0.003 ± 0.009	1.06	0.019	2.17	1.54	2.47	0.167	4
100963	195034	3.762	–0.014 ± 0.019	1.0	0.022	2.17	2.89	1.72	–0.002	3
104075	200746	3.769	0.018 ± 0.107	1.06	0.018	2.11	1.24	2.72	0.051	5
109110	209779	3.766	–0.011 ± 0.031	1.05	0.019	2.14	1.61	2.49	0.071	5
110205	211786	3.756	–0.023 ± 0.035	0.92	0.026	2.19	2.68	1.09	–0.229	1
112504	215696	3.759	0.043 ± 0.041	1.0	0.024	2.22	1.63	2.01	0.007	3
113579	217343	3.76	–0.056 ± 0.025	1.03	0.023	2.24	0.15	3.06	0.054	13
113989	218209	3.741	–0.107 ± 0.015	0.82	0.034	2.25	0.9	<0.83	–0.462	3
115715	220821	3.755	0.072 ± 0.038	0.93	0.027	2.24	1.32	1.72	–0.192	2
116613	222143	3.769	0.010 ± 0.016	1.06	0.019	2.07	4.16	2.12	0.156	2
Sun	–	3.762[a]	0	1.0	0.021	–	–	1.1[a]	–	1.7[b]

Notes. Derived masses, outer convective zone $(1 - Mr/M_{*})$, temperature at the bottom of the convective zone $T_{\rm bcz}$, age, and luminosities for our program stars. [(a)] Grevesse and Sauval (1998). [(b)] Valenti and Fischer (2005).

Figures 5 and 6 show two interesting properties as solar-analog stars. Although the masses of the present sample of solar-analogs appears to span a narrow range of values, namely masses between 0.82 and 1.1 $M_{\odot}$, one observes a strong dispersion in the distribution of lithium abundance versus stellar mass, once finely discretized sets of mass are considered. For masses $M \geq 0.85\ M_{\odot}$, in particular, a wide range of about 2.5 orders of magnitude of A(Li) is observed in Fig. 5, a dispersion also observed at any given mass.

Since convection zone deepening depends primarily on both stellar mass and age, the A(Li) pattern in Fig. 5 should again parallel that observed in Fig. 6, at least in relation to the A(Li) dispersion. A comparison between Figs. 5 and 6 indicates that stars with the smallest masses have the lowest Li

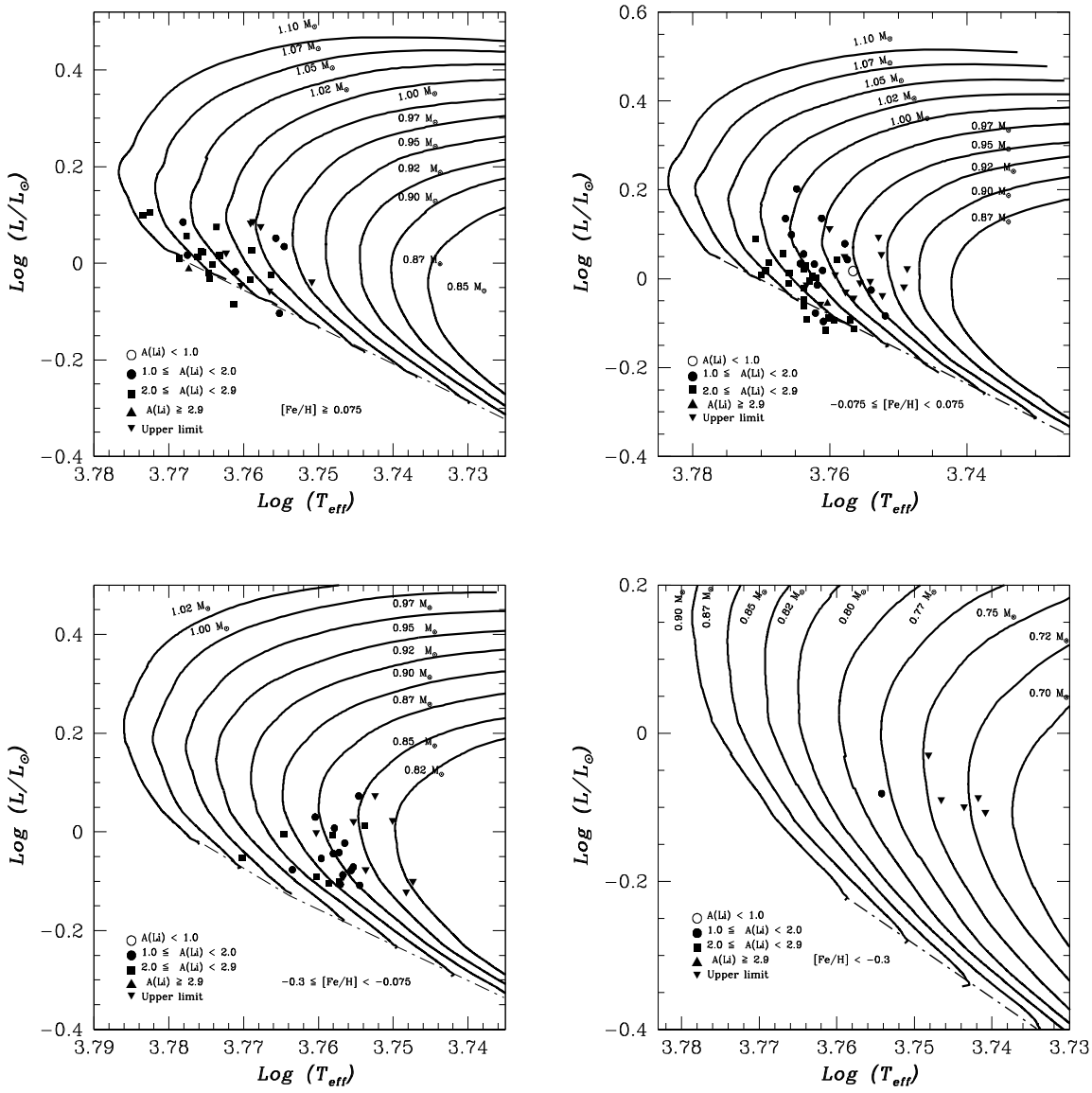

Fig. 4. Distribution of Li abundances in the HR diagram. The different symbols represent Li abundances. Filled inverse triangles represent the upper limits Li to the abundances. Evolutionary tracks, as in Fig. 1.

abundances. This feature reinforces the claim that the root-cause of the low lithium content observed in these stars is primarily related to their previous evolutionary history and that other parameters in addition to stellar mass and metallicity affect the degree of depletion.

3.2. Lithium and rotation relationship in solar-analog stars

The behavior of the rotational velocity is of obvious importance to our understanding of the lithium-rotation relationships in solar-analog stars because it is largely accepted that rotation has a major influence on Li abundances. Different studies, again suggest that the Sun may be an abnormally slow rotator (Lambert & Reddy 2004), compared to similar solar-type disk stars. Unfortunately, there are two major difficulties in this analysis caused by stellar rotational velocity. First, the true rotation of the vast majority of solar-analogs is unknown, because the main detection procedure currently in use gives provides the projected rotational velocity, namely the minimum stellar rotation ($v \sin i$). The definitive rotation rate can only be derived using a photometry procedure. To date, the literature lists the rotational period for only a small percentage of the identified solar-analog stars. For instance, Messina & Guinan (2004) provide the photometric rotation period for 6 apparent solar-analogues, all the stars with periods between 2.6 and 9.21 days rotating more rapidly than the Sun. Unfortunately, only one of these 6 solar-analog stars is listed in the literature. In addition, Butler et al. (1998) measure a period of about 30 d for the solar analog HD 187123. In spite of these difficulties, the preliminary study by Takeda et al. (2007) illustrates that solar analogues with lower rotational velocity ($v \sin i$) also have lower Li abundances. This conclusion is based on measurements of line widths, from which theses authors estimated the $v \sin i$+macroturbulence of each star. This result is confirmed by Gonzalez (2008), using $v \sin i$measurements, separated from the macroturbulence, for a sample of stars with planets.

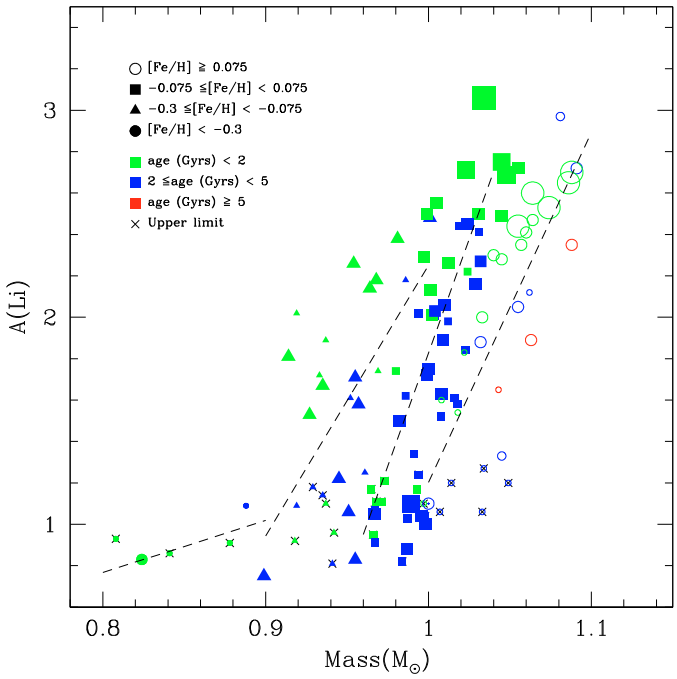

Fig. 5. Lithium abundance as a function of mass (in $M_{\odot}$). Different symbols stand for the following metallicity intervals: open circle [Fe/H] ≥ 0.075, square −0.075 ≤ [Fe/H] < 0.075, triangle −0.3 ≤ [Fe/H] < −0.075, solid circle [Fe/H] < −0.3. Upper limit Li abundances are represented by x. The Sun is also displayed for comparative purposes. The symbol size indicate the projected rotational velocities ($v \sin i$).

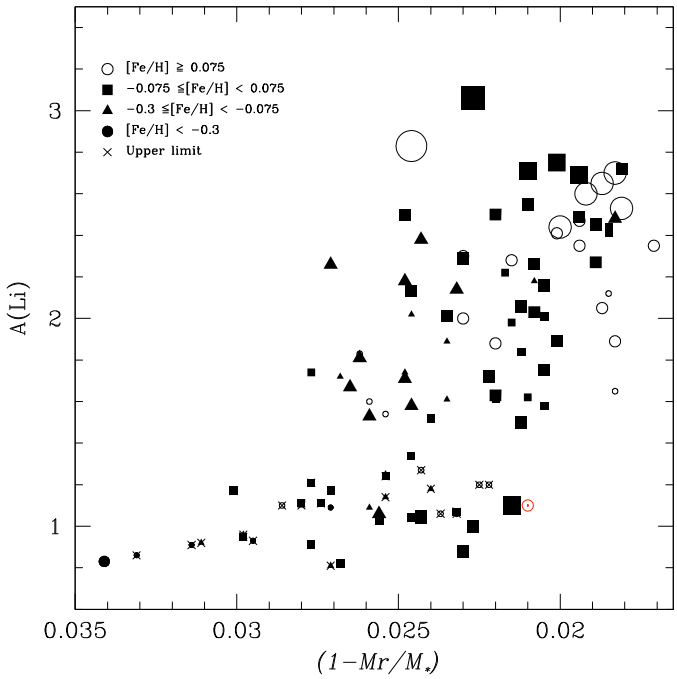

Fig. 6. Lithium abundance as a function of convection zone mass deepening ($1 - Mr/M_{*}$). Stars are grouped into metallicity intervals, as in Fig. 5. Upper limit Li abundances are represented by x. The Sun is also represented for comparative purposes.The symbol size indicate the projected rotational velocities ($v \sin i$).

We now revisit the rotational behavior analyses of solar-analog stars by considering the same sample of solar-analogues studied by Takeda et al. (2007), but now using $v \sin i$ from Nordström et al. (2004), which corresponds to the difference in rotation from the macroturbulence. Figure 7 shows the distribution of the projected rotational velocity ($v \sin i$) in the HR diagram, for the aforementioned stellar sample, with evolutionary tracks computed in the scope of the present work. We can clearly observe, an important scatter in the distribution of $v \sin i$ with mass, in particularly among stars of mass ≥0.95 $M_{\odot}$. For more massive stars, one also observes significant scatter in $v \sin i$ at a given mass. This latter result implies that parameters others than stellar mass and $T_{\rm eff}$ may also be controlling the rotation of solar-analog stars.

The strong dispersion in A(Li) at a given stellar mass or convection zone depth, for $(1 - Mr/M_{*}) \leq 0.03$ and mass >0.9 $M_{\odot}$, as shown in the previous section, indicates that Li depletion depends on parameters other than stellar mass, such as age and early rotational history. To analyze in detail the role of rotation and age in this context, we illustrate in Fig. 5 the distribution of A(Li) versus mass, with the stars segregated by metallicity, age, and $v \sin i$. First, it is clear that solar-analogs show the same trends between lithium content and rotation observed for other stellar families, where the largest $v \sin i$ is associated with the largest A(Li). For instance, except for one star, HD 166435 (HIP 88945), all the stars with enhanced rotation exhibit a large A(Li). In contrast, among slow rotators one observes a large spread in lithium content, from the smallest A(Li) ∼−0.8 to the largest A(Li) ∼3 values. Furthermore, this figure shows an inhabited region for low mass stars, in the sense that for masses lower than about 0.84 $M_{\odot}$, stars with larger A(Li) than about 1 and enhanced rotation seem unusual, a pattern that is clearly associated with stellar age.

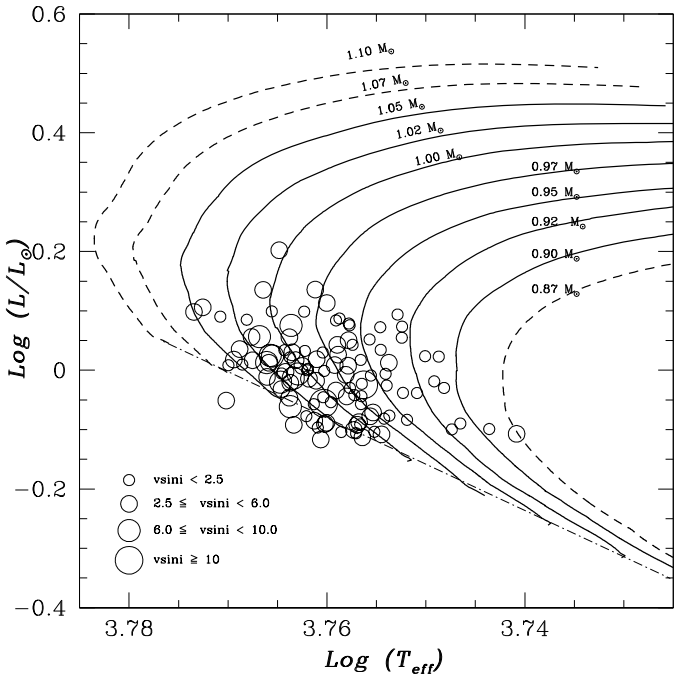

Fig. 7. Distribution of projected rotational velocity measurements ($v \sin i$, in km s^{-1}) in the HR diagram. The different symbols represent the rotational velocities. The evolutionary tracks are similar to those as in Fig. 1.

4. Conclusions

In the past decade, different studies of low-mass stars have provided important information about the physical properties of solar-analog stars. Spectroscopic data have offered important border conditions to choose good candidates, based on

the surface composition of photometrically solar-analog stars. Nevertheless, the important scatter in the distribution of different physical parameters, such as lithium abundance and rotation, indicates, in the broad sense, that information regarding surface convection and angular momentum may be essential to the classification of solar-analog and solar twins stars. To investigate the evolutionary status, mass, and any correlation between Li abundance, convection, and rotation of solar-analog G dwarf stars, we computed a grid of hundreds of evolutionary models for stars of different metallicity and mass range, from 0.7 to 1.1 $M_{\odot}$. These evolutionary tracks were computed using the Toulouse-Geneva code with updated physical inputs, as described in do Nascimento et al. (2009). Our analysis of lithium abundance in a sample of solar-analog stars found different degrees of lithium depletion, a large scatter in the abundance being observed for stars over a narrow range of mass and metallicity. Low Li abundance among solar-analog stars strongly supports the hypothesis that these stars have depleted Li during the MS phases. These results illustrate the need for an extra-mixing process to explain lithium behavior in solar-analog stars, such as, shear mixing caused by differential rotation proposed by Bouvier (1995).

The aforementioned dispersion in the lithium abundance of solar-analog stars at a given age and mass may also reflect their different rotational histories. In spite of the short range of mass in the solar-analog stars, this study shows how sensitive A(Li) scatter is as a function of stellar mass, metallicity, age and, $T_{\rm eff}$. It cannot however be excluded that the Galactic cosmic Li abundance dispersion could contributes to the scattering in lithium abundance. Even if solar-analog stars were chosen according to their spectroscopic and photometric similarity with the Sun, our conclusion in this study reinforces the need for information about the stellar interior. Furthermore, the Li depletion observed in the solar-analog stars and the large spread in Li abundances among the five known solar twins cannot be explained only by standard convective mixing. At a given $T_{\rm eff}$ or age, a small percentage difference in stellar mass, and consequently in the depth (in mass) of the stellar convective envelope, can produce a A(Li) scatter, which tends to increase with stellar mass and $T_{\rm eff}$. This illustrates that in producing a more realistic definition of solar-analog and solar-twin stars, it seems important to consider the inner physical properties of stars, such as the depth of the convective envelope mass and consequently rotation and magnetic properties. Finally, we note that asteroseismology offers a unique opportunity to study the extension of outer convection zones of solar-analogs. This study and a determination of the chemical abundance pattern of solar-analog and solar-twins stars could play an important role in answering the fundamental question about how normal the Sun as a star really is.

Acknowledgements. This research made use of the SIMBAD data base, operated at CDS, Strasbourg, France. J.D.N. and J.R.M. are research fellows of the CNPq Brazilian agency. Research activities of the Stellar Board at the Federal University of Rio Grande do Norte are supported by continuous grants from CNPq and FAPERN Brazilian Agencies. We thank the anonymous referee for the useful comments and suggestions.

References

Alexander, D. R., & Ferguson, J. W. 1994, ApJ, 437, 879
Angulo, C., Arnould, M., & Rayet, M. 1999, Nucl. Phys. A, 656, 1
Bahcall, J. N., & Pinsonneault, M. H. 1992, RvMP, 64, 885
Bouvier, J. 2008, A&A, 489, L53
Böhm-Vitense, E. 1958, ZAp, 46, 108
Butler, R. P., Marcy, G. W., Vogt, S. S., & Apps, K. 1998, PASP 110. 1389
Cayrel de Strobel, G. 1996, A&ARv, 7, 243
do Nascimento, J. D. Jr., Charbonnel, C., Lébre, A., de Laverny, P., & De Medeiros, J. R. 2000, A&A, 357, 931
do Nascimento, J.-D., Jr., Castro, M., Meléndez, J., et al. 2009, A&A, 501, 687
ESA 1997, The Hipparcos and Tycho Catalogues, ESA SP-1200
García López, R. J., Rebolo, R., & Beckmann, J. E. 1988, PASP, 100, 1489
Girardi, L., Bressan, A., Bertelli, G., & Chiosi, C. 2000, A&AS, 141, 371
Gonzalez, G. 2008, MNRAS, 386, 928
Grevesse, N., & Noels, A. 1993 in Origin and Evolution of the Elements, ed. N. Prantzos, E. Vangioni-Flam, & M. Cassé (Cambridge: Cambridge University Press), 15
Grevesse, N., & Sauval, A. J. 1998, Space Sci. Rev., 85, 161
Holmberg, J., Nordström, B., & Andersen, J. 2007, A&A, 475, 519
Hui-Bon-Hoa, A. 2007, Ap&SS, 340
Iglesias, C. A., & Rogers, F. J. 1996, ApJ, 464, 943
Jones, B. F., Fisher, D., & Soderblom, D. R. 1999, AJ, 117, 330
King, J. R., Boesgaard, A. M., & Schuler, S. C. 2005, AJ, 130, 2318
Lambert, D. L., & Reddy, B. E. 2004, MNRAS, 349, L757
Messina, S., & Guinan, E. 2004, A&A, 428, 983
Meléndez, J., & Ramirez, I. 2007, ApJ, 669, L89
Meléndez, J., Dodds-Eden, K., & Robles, J. A. 2006, ApJ, L641, 133
Nordström, B., Mayor, M., Andersen, J., et al. 2004, A&A, 418, 989
Paquette, C., Pelletier, C., Fontaine, G., & Michaud, G. 1986, ApJS, 61, 177
Pasquini, L., Randich, S., & Pallavicini, R. 1997, A&A, 325, 535
Pasquini, L., Biazzo, K., Bonifacio, P., Randich, S., & Bedin, L. R. 2008, A&A, 489, 677
Porto de Mello, G. F., & Da Silva, L. 1997, ApJ, 482, L89
Randich, S. 2006, in Chemical Abundances and Mixing in Stars in the Milky Way and its Satellites, ed. S. Randich, & L. Pasquini (Springer-Verlag), 173
Richard, O., Vauclair, S., Charbonnel, C., & Dziembowski, W. A. 1996, A&A, 312, 1000
Richard, O., Théado, S., & Vauclair, S. 2004, Sol. Phys., 220, 2, 243
Rogers, F. J., & Nayfonov, A. 2002, ApJ, 576, 1064
Soderblom, D. R., Stauffer, J. R., Hudon, J. D., & Jones, B. F. 1993, ApJS, 85, 313
Spite, F., Spite, M., Peterson, R. C., & Chaffee, F. H. Jr. 1987, A&A, 171, L8
Takeda, Y., Kawanomoto, S., Honda, S., Ando, H., & Sakurai, T. 2007, A&A, 468, 663
Valenti, J., & Fischer, D. 2005, ApJS, 159, 141